UK Atomic
Energy
Authority

UKAEA-STEP-CP(23)08

Daniel Kennedy Bhavin S Patel Colin M Roach

Microtearing Modes in high-β Spherical Tokamaks

Microtearing Modes in high-β Spherical Tokamaks

Daniel Kennedy Bhavin S Patel Colin M Roach

Microtearing Modes in high-β Spherical Tokamaks

D. Kennedy[1], B.S. Patel[1], and C. M. Roach[1]

[1] *Culham Centre for Fusion Energy Abingdon, Oxfordshire, OX14 5EB, UK*

Microinstabilities often result in turbulence that influences energy confinement in tokamak discharges. One such microinstability, of particular importance to the design of next-generation spherical tokamaks (STs) such as STEP [1], is the microtearing mode (MTM).

MTMs tear equilibrium flux surfaces and are driven on rational surfaces primarily by the electron-temperature gradient R/L_{Te}. MTMs are electromagnetic modes which propagate in the electron diamagnetic direction. In STEP-like equilibria, we find that MTMs can be unstable over a wide range of binormal scales (see Fig. (1)). At $k_y \rho_i \ll 1$ (▲), MTMs are often sub-dominant to KBMs, and MTM eigenfunctions in ϕ are highly extended in ballooning space (i.e. access high k_x). At $k_y \rho_i \geq 1$ (■), the MTM eigenfunctions in ϕ are highly ballooning and localised about $\theta = 0$. We are particularly concerned by MTMs at $k_y \rho_s \ll 1$ (▲), as these low k_y MTMs are more weakly affected by flow shear and tend to dominate large fluxes at late times in nonlinear simulations.

Figure 1: *Growth rate and frequencies of the dominant odd and even parity micro-instabilities as a function of $k_y \rho_s$ with $\theta_0 = 0$ for the $\rho_\psi = 0.5$ surface of the baseline equilibrium calculated by GS2. Figure adapted from [1].*

In STEP-like parameter regimes, nonlinear gyrokinetic (GK) simulations tend to either: (i) reach a quasi-saturated state at where the associated fluxes far exceed experimental operating limits; or (ii) fail to saturate entirely. Local GK simulations of type (i) tend to be accompanied by an unphysical end-state with box-scale turbulent structures that cannot be accurately described within the local GK framework, so it is therefore unclear whether the runaway and/or large flux saturated states are physical.

Predictions of the performance of future ST fusion plants require reliable models that can describe MTM driven turbulent transport. In this short paper, we explore two paths towards progress on this front: (A) progress on reduced models of MTM-driven electron thermal transport; and (B) progress on global GK simulations of MTMs.

(A) Reduced models of MTM turbulence

One such reduced model [2], hereinafter the RAFIQ model, has been successful at modelling experimental discharges in NSTX and reproducing the trends predicted by GK simulations [3]. In the RAFIQ model, the MTM electron thermal diffusivity is computed according to the Rechester–Rosenbluth model [4] and, in principle, the entire spectrum of magnetic fluctuations is needed to calculate the heat flux. However, [2]
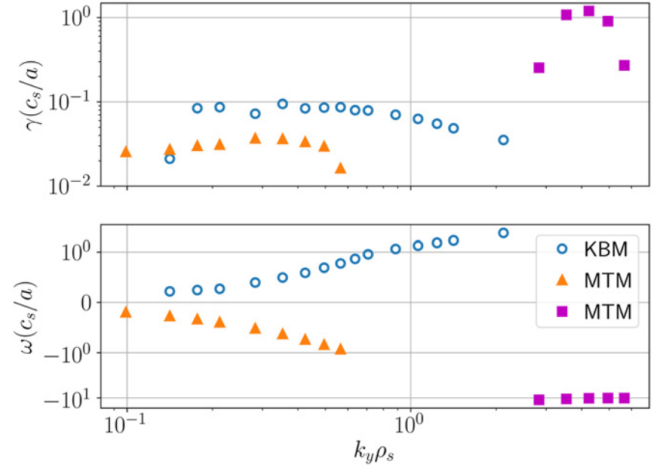
argues that the use of most unstable linear MTM is sufficient and thus the real workhorse of the RAFIQ model is the dispersion relation used to calculate the growth rate of the fastest growing unstable MTM.

Unfortunately, despite successfully modelling MTM-dominated discharges in existing experiments (e.g., [3]), we find that the linear solver (i.e., the linear limit of the dispersion relation in [2]) in the RAFIQ model does a poorer job of capturing linear MTMs in a STEP-like equilibria (see Fig. (2)). In order to try to pinpoint where the RAFIQ model might be failing we developed an IN HOUSE model making similar physics assumptions to RAFIQ, but avoiding approximations that may not be valid for MTMs in STEP-like plasmas (we avoid using a cut-off to approximate velocity space integrals).

Our starting point is the linear electron gyrokinetic equation

$$\left(\omega - k_\parallel v_\parallel - \omega_{De}(v_\parallel^2, v_\perp^2) + i\nu(v)\right)\left(f_k - \frac{e\phi}{T_e}f_0\right) = -\frac{e}{T_e}(\omega - \omega_{\star e}(v))(\phi - v_\parallel A_\parallel)f_0. \quad (1)$$

As usual, the subscript $\parallel$ ($\perp$) refers to the component of a vector parallel (orthogonal) to a unit vector in the direction of the magnetic field $\boldsymbol{b} = \frac{\boldsymbol{B}}{B}$, e.g., $v_\parallel = \boldsymbol{b} \cdot \boldsymbol{v}$, $\boldsymbol{v}_\perp = \boldsymbol{v} - v_\parallel \boldsymbol{b}$, where $\boldsymbol{B}$ is the magnetic field, $\boldsymbol{v}$ is the electron velocity, and f_0 is the equilibrium Maxwellian distribution function $f_0 = \frac{n_e}{\pi^{3/2}v_{\text{the}}^3}\exp\left(-\frac{v^2}{v_{\text{the}}^2}\right)$, $v_{\text{the}}^2 = \frac{2T_e}{m}$. As usual, we also have defined the diamagnetic drift frequency $\omega_{\star e}(v) = \omega_{\star e}\left[1 + \eta_e\left(v^2 - \frac{3}{2}\right)\right]$, $\omega_{\star e} = \frac{k_y T_e g_{ne}}{eBR}$, with $g_{ne} = -R\boldsymbol{e}_x \cdot \nabla n_e/n_e$, $g_{Te} = -R\boldsymbol{e}_x \cdot \nabla T_e/T_e$, $\eta_e = \frac{g_{Te}}{g_{ne}}$, and the magnetic drift frequency $\omega_{De}(v_\parallel^2, v_\perp^2) = \boldsymbol{k} \cdot \boldsymbol{v}_{De}$, $\boldsymbol{v}_{De} = \frac{T_e}{m_e \Omega_i}\boldsymbol{b} \times \left(\frac{\nabla B}{B} + \boldsymbol{b} \cdot \nabla \boldsymbol{b}\right)$. In Eq. (1), the perturbed distribution function is written as $f_k = \delta f \equiv g + \frac{e\phi}{T}f_0$, where g is the gyrophase-independent part of the distribution function.

Rearranging (1) yields

$$f_k = \frac{e\phi}{T_e}f_0 - \left(\frac{e\phi}{T_e} - v_\parallel \frac{eA_\parallel}{T_e}\right)\left(\frac{\omega - \omega_{\star e}(v)}{\omega - k_\parallel v_\parallel - \omega_{De}(v_\parallel^2, v_\perp^2) + i\nu(v)}\right)f_0. \quad (2)$$

As discussed previously, we are mostly concerned with the collisional MTM at $k_y \rho_i \ll 1$ with very low $k_\parallel$. As such, we can neglect $k_\parallel$. Armed with this assumption, substituting Eq. (2) into Ampére's law $j_\parallel \equiv -\int ef_k v_\parallel \, d^3\mathbf{v} = \frac{1}{\mu_0}k_\perp^2 A_\parallel$, and rescaling $x \equiv \frac{v}{v_{\text{the}}}$, $d^3\boldsymbol{v} = 2\pi v_{\text{the}}^3 x_\perp \, dx_\parallel dx_\perp$, we obtain the dispersion relation

$$F(\omega_r, \gamma; k_\perp) \equiv \frac{1}{\mu_0}k_\perp^2 + \frac{2e^2 n_e v_{\text{the}}^2}{T_e \sqrt{\pi}}\int_0^\infty \int_{-\infty}^\infty x_\parallel^2 x_\perp \frac{\omega - \omega_{\star e}\left[1 + \eta_e\left(x^2 - \frac{3}{2}\right)\right]}{\omega - \omega_{De} + i\nu(x)}\exp(-x^2)\,dx_\parallel dx_\perp = 0. \quad (3)$$

A Python script is used to find the zeros of the function F[1], and we use the approximations in [2] to evaluate ω_{De} and ν. In Fig. (2) we compare the results of the RAFIQ and IN HOUSE models against local GK (CGYRO) in two ST geometries. It appears that RAFIQ is the better model for NSTX, but the IN HOUSE calculation is better for STEP! We are working on developing reduced models for the different classes of MTMs that appear at low and high k_y in STEP-like plasmas, including an assessment of the MTM susceptibility to stabilisation by sheared flows.

(B) Global simulations of MTMs

In the absence of experiments close to STEP-like parameters, the litmus test for reduced models will be whether we can benchmark reduced models against saturated nonlinear GK simulations.
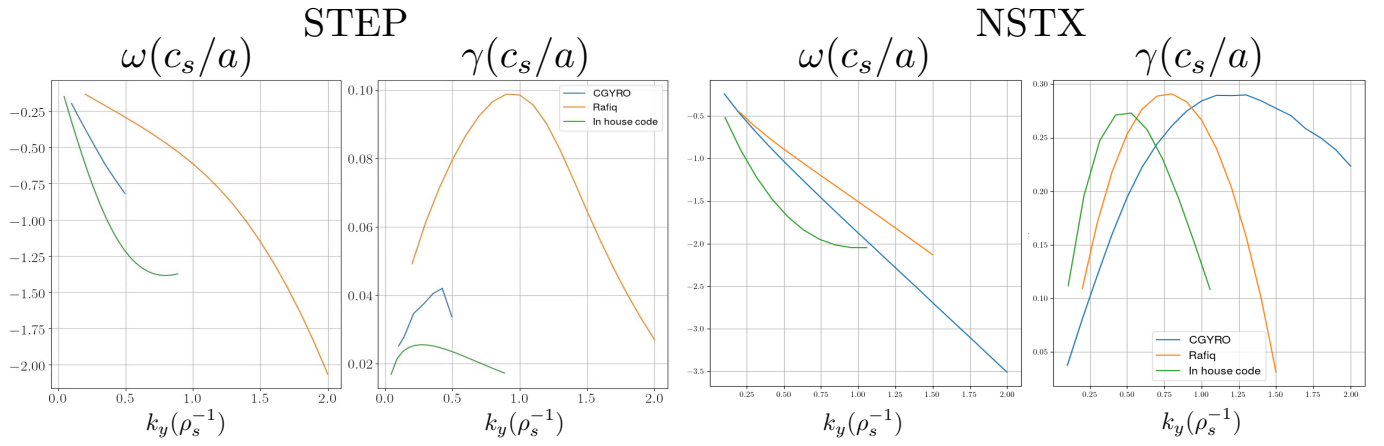
---

[1]see https://github.com/bpatel2107/mtm_solver.

Figure 2: *Comparison of existing linear models (RAFIQ [2], and IN HOUSE solution of Eq. (3)) and local GK (CGYRO) calculations for two different ST geometries STEP [1] (LHS) and NSTX [3] (RHS).*

In Fig. (3), we show the results of a generic, local 2-field GK simulation $(\delta\phi, \delta A_{\parallel})$ for a STEP-like case ([1]) with $a/L_{Ti} = 0$. Whilst the simulation reaches a quasi-saturated state, the predicted heat flux greatly exceeds the available power. Moreover, this quasi-saturated state is accompanied by box-scale radial streamers (i.e., an unphysical end state). This result, which is not atypical, departs from the domain of validity of local GK, and suggests value in pursuing a global approach.

To understand the impact of global effects at low poloidal mode number n, we perform global simulations using the GK code GENE [5]. As a first step

Figure 3: *Time evolution of the heat flux (LHS) and contour plots of the electrostatic ϕ and magnetic $A_{\parallel}$ vector potentials (RHS) at the final time step in a nonlinear STEP simulation.*

in this direction, we aim to compare global GK against local GK in the high n limit. The calculations for this benchmark were performed in a STEP-like equilibrium with lower β_e than that used in the local calculations above. local GK at $\rho_{\psi} = 0.5$ predicts that this equilibrium is KBM dominated, with subdominant unstable MTM, at low $k_y\rho_i$. When attempting this benchmark, we discovered that the maximum radial resolution is limited by the resolution of the numerical equilibria. For a numerical STEP equilibrium with $(NR, NZ) = (1600, 1600)$, we find that the radial resolution should be limited to: $\Delta\rho_{\text{tor}} \geq \Delta^{\star} \approx 2 \times 10^{-3}$. Resolving rational spacing Δ_{rat} requires: $\Delta^{\star} < \Delta_{\text{rat}}$, and thus requiring 20 points between rational surfaces for the equilibrium region studied requires $n < 50$.

The results of this first linear benchmark are shown in Fig. (4). As expected, the growth rates calculated by the local and global codes appear to converge as n increases up the scales which we can confidently resolve. However, a caveat to this is that it appears the local and global codes identify different instabilities as the most unstable mode (note sign of real frequency). Unsurprisingly, global physics appears to play a
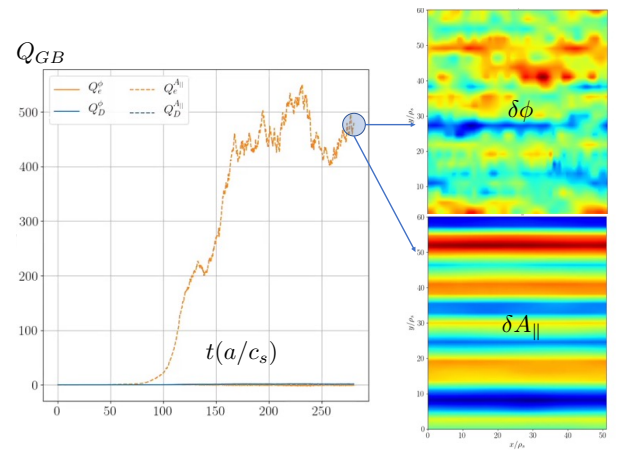
role at low *n* where the local and global calculations diverge, and where there is a larger variation of the temperature and density gradients across the radial box (see inset).
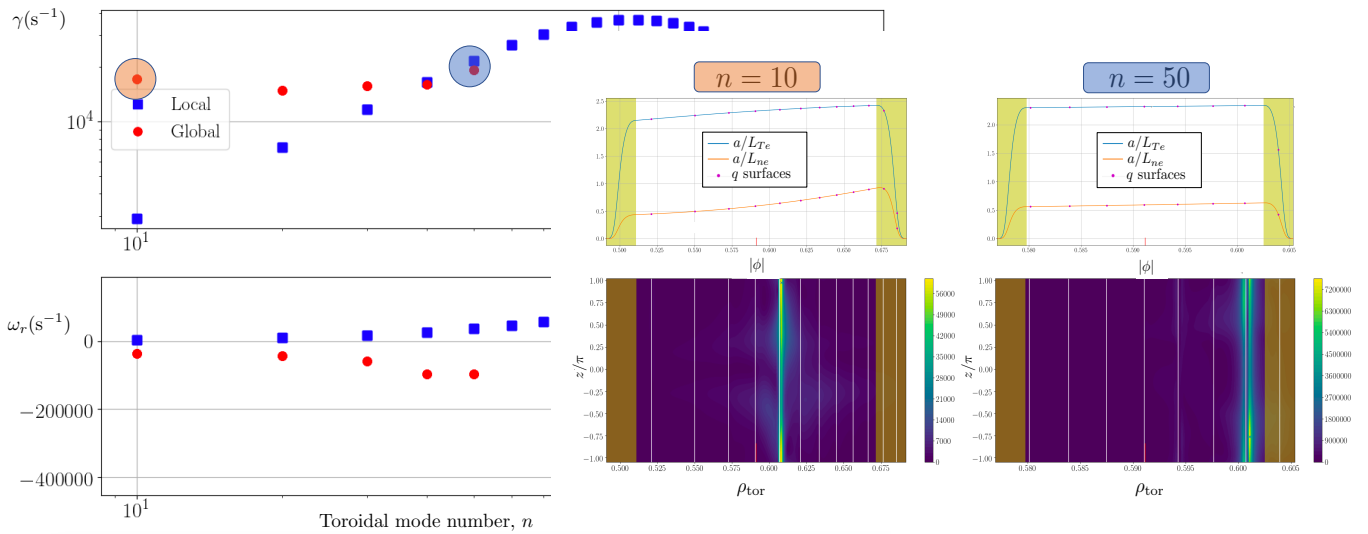

Figure 4: *Comparison of LOCAL and GLOBAL GK calculations. Shown is the growth rate γ and real frequency ω$_r$ of the fastest growing linear mode as a function of toriodal mode number n in a STEP-like equilibria. On the right-hand inset, the variation of the temperature and density gradients (top) are shown alongside the global mode structure |φ|(x, z)|. (bottom). The buffer regions (where a Krook operator is employed in the global simulations) are shown as a shaded yellow region. The rational surfaces are shown as dots (top) and white lines (bottom).*

Conclusions

Understanding the physics of MTMs, and in particular their nonlinear saturation or lack thereof, is a key challenge in the design of next-generation STs. We have found that existing reduced models can approximately match local GK linear properties for some classes of MTM in some ST equilibria, but more effort is needed to improve the models and their breadth of scope. We have also found that global effects are significant at low *n* in STEP, and we will carry out global simulations to investigate STEP-like equilibria where local GK simulations of low *n* MTMs fail to saturate with acceptable fluxes.

References

[1]   B.S. Patel et al. "Linear gyrokinetic stability of a high *β* non-inductive spherical tokamak". In: *Nuclear Fusion* 62.1 (2021), p. 016009. DOI: 10.1088/1741-4326/ac359c. URL: https://doi.org/10.1088/1741-4326/ac359c.

[2]   T. Rafiq et al. "Microtearing modes in tokamak discharges". In: *Physics of Plasmas* 23.6 (2016), p. 062507. DOI: 10.1063/1.4953609. eprint: https://doi.org/10.1063/1.4953609. URL: https://doi.org/10.1063/1.4953609.

[3]   T. Rafiq et al. "Microtearing instabilities and electron thermal transport in low and high collisionality NSTX discharges". In: *Physics of Plasmas* 28.2, 022504 (Feb. 2021), p. 022504. DOI: 10.1063/5.0029120.

[4]   A. B. Rechester and M. N. Rosenbluth. "Electron Heat Transport in a Tokamak with Destroyed Magnetic Surfaces". In: *Phys. Rev. Lett.* 40 (1 1978), pp. 38–41. DOI: 10.1103/PhysRevLett.40.38. URL: https://link.aps.org/doi/10.1103/PhysRevLett.40.38.

[5]   T. Görler et al. "The global version of the gyrokinetic turbulence code GENE". In: *Journal of Computational Physics* 230.18 (2011), pp. 7053–7071. ISSN: 0021-9991. DOI: https://doi.org/10.1016/j.jcp.2011.05.034. URL: https://www.sciencedirect.com/science/article/pii/S0021999111003457.